Int. Journal of Refractory Metals and Hard Materials 47 (2014) 93–101

Contents lists available at ScienceDirect

Int. Journal of Refractory Metals and Hard Materials

journal homepage: www.elsevier.com/locate/IJRMHM

Effects of Fe additions on self propagating high temperature synthesis characteristics of TiO_2–Al–C system

M. Sharifitabar, J. Vahdati khaki *, M. Haddad Sabzevar

Department of Metallurgical Engineering, Faculty of Engineering, Ferdowsi University of Mashhad, P.O. Box 91775-1111, Mashhad, Iran

ARTICLE INFO

Article history:
Received 5 May 2014
Accepted 2 July 2014
Available online 9 July 2014

Keywords:
Self propagating high temperature synthesis
TiO_2–Al–C–Fe system
Raman analysis
TiC growth mechanism

ABSTRACT

The aim of the present study was to investigate the effect of Fe additions on combustion velocity and phases that are formed after synthesis in the TiO_2–Al–C system. Before experimental tests, thermodynamic calculations were performed to determine the range that Fe can be added to the reaction and remain self sustaining. According to the Merzhanov criterion, if the amount of Fe is lower than 53.13 wt.%, the adiabatic temperature of the reaction is higher than 1800 K and therefore the reaction proceeds in the self sustaining mode. But, experimental observations showed that the reaction became unstable when the amount of Fe was changed from 15 to 20 wt.%, which was considerably lower than that was predicted by thermodynamic calculations. X-ray diffraction analysis indicated that Fe_3Al, TiC and Al_2O_3 are the main phases formed in the products and additions of Fe decreased the lattice parameter of TiC. Also, Raman spectroscopy analysis showed that at higher Fe contents, oxygen dissolved in the TiC crystal structure leading to the formation of titanium oxy-carbide with lower lattice parameter and residual un-reacted carbon in the products. The adiabatic temperatures for the reactions containing 15 and 20 wt.% Fe estimated using the thermodynamic data of the new products were in conformance with the Merzhanov criterion and experimental observations. Scanning electron microscopy examinations showed that the addition of Fe decreased TiC particle size and changed their growth controlling mechanism.

Introduction

The particle reinforced metal-matrix composites are a group of materials which can be used in wear and corrosion resistance applications because of their low costs, the ease of fabrication, high stiffness and elastic modulus and isotropic properties [1,2]. Despite of the higher density of iron base composites, their lower output costs and more isotropic properties make these materials attractive for many applications. The types of reinforcements, their compatibility with the matrix and their volume fraction have considerable effects on the properties of these composites [3]. Among all ceramic reinforcing particles, titanium carbide (TiC) due to its outstanding properties including high melting point (3250 °C), high hardness (2890–3200 HV), low density (4.93 g/cm^3), high elastic modulus (269 GPa), excellent corrosion resistance and good thermodynamic stability with the Fe melt is a proper candidate for fabricating Fe based composites [1,4].

The combustion synthesis process is a low cost and quick process for the production of different ceramics, ceramic matrix and metal matrix composites [5–8]. This procedure usually is divided into two different categories called volume combustion synthesis (VC) and self propagating high temperature synthesis (SHS). During VC, samples are heated uniformly to the reaction initiation temperature. Then, the reaction starts in all parts of the sample simultaneously. But, in SHS process, a small part of a sample is heated by a localized heat source like a tungsten filament. Once the reaction starts, the heat liberated provides the necessary heat for its propagation along the entire sample. Lower costs and simplicity are the advantages of SHS over volume combustion [8].

Fabrication of TiC and composites containing this compound by the SHS process was the main topic of many researches [5–7,9–18]. Among different combustion reactions, reduction of titanium oxide (TiO_2) with aluminum in the presence of carbon is an exothermic reaction which goes to the formation of a composite which consists of TiC and aluminum oxide (Al_2O_3). This reaction, which usually is called aluminothermic reduction of TiO_2 is as follows:

$$3TiO_2 + 4Al + 3C \rightarrow 3TiC + 2Al_2O_3 \quad \Delta H_{298} = -1072.7 \text{ kJ}. \tag{1}$$

If a metallic element is added to this reaction and it only acts as a diluent agent, different metal matrix composites consisting of TiC and Al_2O_3 particles as reinforcements can be created. Xia and others [17] produced Al–TiC–Al_2O_3 composite by adding excess Al to reaction 1. They showed that the critical molar ratio of excess aluminum, which the combustion reaction can self-sustain with a preheat temperature of 400–500 K is 7.66 mol. Zhu and co-workers [18] controlled C/TiO_2 molar ratio to fabricate different composites including Al_3Ti–Al_2O_3,

* Corresponding author. Tel.: +98 5518805107.
E-mail address: vahdati@um.ac.ir (J. Vahdati khaki).

http://dx.doi.org/10.1016/j.ijrmhm.2014.07.006
0263-4368/

Al_3Ti–Al_2O_3–TiC and Al_2O_3–TiC. Recently some attempts have been performed for fabricating Fe–TiC–Al_2O_3 composite from ilmenite concentrations by carbo-aluminothermic reduction process [3,19]. But, there is no report on the effect of Fe additions to the aluminothermic reduction of TiO_2 in the open literature. So, in the present work we added various amounts of Fe to reaction 1 and investigated the effect of this parameter on combustion velocity, microstructure and phases that are formed after SHS.

Thermodynamic calculations

The aluminothermic reaction of titanium oxide in the presence of iron considered in the present work is as follows:

$$3TiO_2 + 4Al + 3C + x\text{Fe} \rightarrow 3TiC + 2Al_2O_3 + x\text{Fe}. \quad (2)$$

According to thermodynamic data, in the absence of Fe, the enthalpy of this reaction is extremely negative and hence it is considerably exothermic, but the addition of iron decreases the heat released from this reaction. So, before experimental investigations, thermodynamic calculations were performed to determine the range that iron can be added to reaction 2 (x) and still it will remain self-sustaining.

In exothermic reactions, if the conditions are assumed to be adiabatic, the heat liberated from the reaction can increase the final temperature of the wares. The highest temperature that a reaction system can reach is adiabatic temperature (T_{ad}) and can be calculated using the following formula [7]:

$$-\Delta H^0_{298} = \int_{298}^{T_{tr}} nC_p(\text{products})dT + n\Delta H_{tr} + \int_{T_{tr}}^{T_{ad}} nC_p(\text{products})dT \quad (3)$$

ΔH^0_{298} is the difference between the formation of molar enthalpy of the products and raw materials at 298 K, n is the mole of each product and C_p is the molar heat capacity. If there is any phase change in products during heating, it should be considered in the calculations. So, in the previous formula, T_{tr} is the transformation temperature and ΔH_{tr} is the molar enthalpy of transformation. Also, if a material is added to the reaction as diluents, its heat capacity should be added to the product's heat capacity. Combustion wave stability is dependent on the heat generation by the reaction and heat dissipation to the surrounding area and remaining reactants. The low adiabatic temperature of a reaction indicates that the heat generated by this reaction is low and therefore this reaction cannot propagate in a stable mode [8]. According to the experimental criterion of Merzhanov [8,9], in an exothermic reaction if the calculated adiabatic temperature is higher than 1800 K, it can be self-sustaining and the process is called self propagating high temperature synthesis (SHS). The effect of Fe additions on the adiabatic temperature of reaction 2 is shown in Fig. 1. Also, thermodynamic data used for calculating the adiabatic temperature is presented in Table 1. According to Fig. 1, adiabatic temperature of the aluminothermic reaction of titanium oxide is 2371 K and addition of iron decreases it with a non-uniform trend. The two steps at 2325 K and 1809 K are associated with the melting of alumina and iron, respectively. According to thermodynamic calculations, if the iron added to the reaction is lower than 53.13 wt.%, adiabatic temperature is higher than 1800 K and it is expected that the reaction will be self-sustaining.

Material and methods

Materials

The raw materials used for combustion synthesis were titanium oxide (TiO_2 Anatas, purity higher than 99.5%, <45 μm), activated carbon (Merck, 102184), fine aluminum powder (Rankem, A2265) and iron powder (purity higher than 99 wt.%, <200 μm). According to the above calculations, the amounts of Fe added to the reaction were between 0 and 60 wt.%. Before SHS, these raw materials were mixed in a planetary ball mill for 30 min with a ball to powder ratio of 10:1 using stainless steel balls to produce a homogenous mixture. Then, the mixtures were pressed in a tool steel die and cylindrical compacts with 14 mm diameter, 21–22 high and 57–59% of theoretical density were prepared.

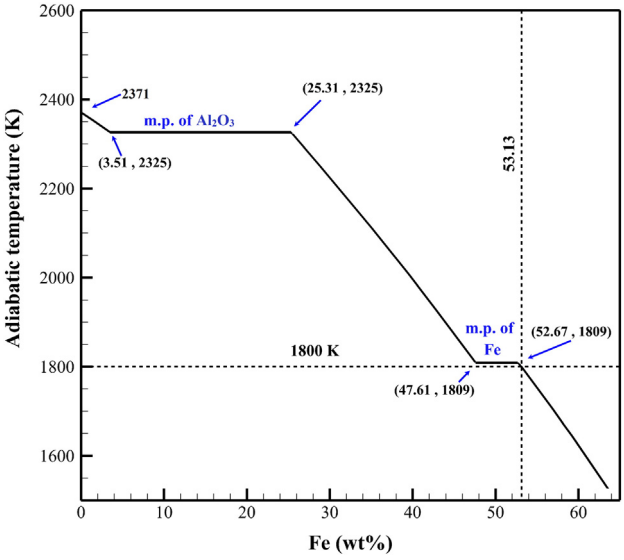

Fig. 1. Effect of Fe additions on adiabatic temperature of reaction 2.

Experimental procedure

The combustion synthesis process was performed in argon atmosphere with purity higher than 99 wt.%. Fig. 2 shows a schematic representation of SHS chamber. Prior to SHS, the argon gas was purged into the chamber with a flow rate of 6 l/min for 3–4 min to ensure that the air in the container is minimized. Also, during synthesis and cooling of samples, the gas flow rate was kept constant at 4 l/min. The necessary heat for ignition of the reaction was provided by passing a 170 A electrical current through a tungsten rod with 1.6 mm in diameter placed 2–3 mm above the green compacts. The synthesis process progression was recorded by a digital camera with a speed of 25 frames/s and the combustion velocity was calculated by dividing the high of the sample to its time of synthesis.

To characterize the reaction products, X-ray diffraction (XRD) analysis was performed with Cu K_α radiation. Raman spectroscopy was performed using a dispersive Raman microscope with a confocal depth resolution of 2 μm, spectral resolution of $<3\ cm^{-1}$ and spectral range between 160 and 3500 cm^{-1} by 785 nm laser. Spectra were taken from different points of the samples to determine the homogeneity and to identify various compounds formed in the samples. Also, microstructures of the products were studied using a scanning electron microscope (SEM, Cambridge S360).

Results

SHS characteristics

Fig. 3a–c shows ignition, propagation and ending of the SHS reactions in samples containing 0, 15 and 30 wt.% Fe, respectively. When there was no Fe in the aluminothermic reaction of titanium oxide, it started after a short period of heating (about 6 s) and propagated quickly along the entire sample with a macroscopic flat front (Fig. 3a). The addition of 15 wt.% Fe to the reaction raised the reaction initiation and propagation times and converted the flat front to wavy

Table 1
Thermodynamic data of different elements and compounds.

Element or compound	Temp. range (K)	ΔH^0 (kJ/mol)	ΔH_m (kJ/mol)	C_p (J/K·mol)
TiC[a]	298 ~ 3290	−184.5		$48.43 + (3.16 \times 10^{-3} \times T) - (1.36 \times 10^{5} T^{-2}) + (1.23 \times 10^{-6} \times T^{2}$
Al_2O_3[a]	298 ~ 2325	−1675.7		$117.49 + (10.38 \times 10^{-3} \times T) - (37.11 \times 10^{5} T^{-2})$
	Liq		107.0	184.10
TiO_2[a]		−944.2		–
Fe[b]	298–1184		α → = 0.9	$12.29 + (37.7 \times 10^{-3} \times T)$
	1184–1665		→ δ = 0.8	$23.99 + (8.36 \times 10^{-3} \times T)$
	1665–1809		δ → = 13.8	$24.64 + (9.90 \times 10^{-3} \times T)$
	Liq			46.02
Fe_3Al	298–1130	−66.93 [20]	13.5	$13.67 + 2.9 \times 10^{-3} \times T$ [21]
	Liq			41.74[c]
C[b]	298–1100	0		$4.3 + 17.8 \times 10^{-3} \times T$
	1100–4100	0		$21,743 + 1.2 \times 10^{-3} \times T$

[a] Ref. [22].
[b] Ref. [23].
[c] Neumann–Kopp rule: $C_{p,\ Fe-25Al} = 0.75C_{p,\ Fe} + 0.25C_{p,\ Al}$ [24].

one (Fig. 3b). But, in the sample with 30 wt.% Fe, the reaction only happened in a thin surface layer after a long heating time and then it ended without further propagation (Fig. 3c). This experimental observation was in contrary with the theoretical calculations which predicted that the reaction will be self-sustaining in all samples containing Fe lower than about 53 wt.%. So, in the second experiment, samples containing 0–30 wt.% Fe with 5 wt.% intervals were prepared for SHS. Fig. 4 shows the simultaneous effects of Fe addition on combustion velocity and adiabatic temperature. Addition of iron to the reaction from 5 to 15 wt.% decreased the combustion velocity of the reaction considerably, but in the sample containing 20 wt.% Fe, the reaction did not propagate along the entire sample and quenched before reaching to the end of it. So, it can be concluded that the addition of Fe from 15 to 20 wt.% led to the instability of the reaction. The adiabatic temperature for reaction 2 with 15 and 20 wt.% Fe is 2325 K which is considerably higher than the Merzhanov criterion (1800 K). This criterion is based on experimental results and it is verified in many SHS reaction systems [8]. So, to reveal the reason(s) why it is not applicable for reaction 2, phase analysis was performed on the products to investigate the effect of iron addition on phases formed after combustion.

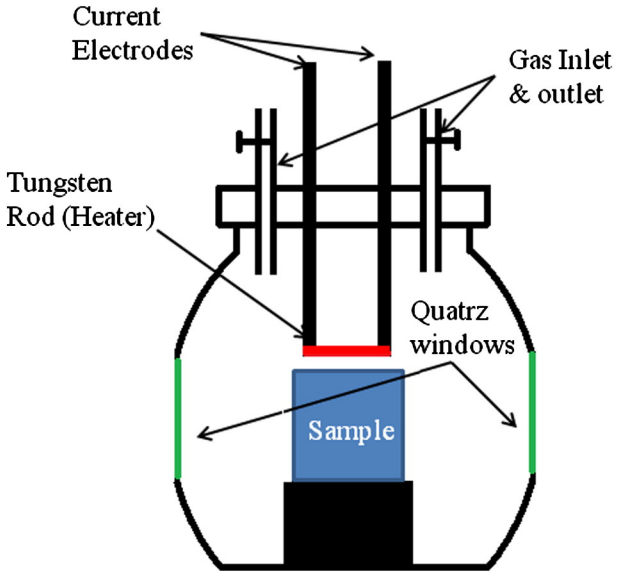

Fig. 2. Schematic representation of SHS chamber.

Phase analysis

XRD analysis

XRD analysis of the samples which contains 0 to 20 wt.% Fe is demonstrated in Fig. 5. The only phases formed in the sample with no Fe are titanium carbide (TiC, ICDD card no. 00-003-1213) with a cubic crystal structure and aluminum oxide (α-Al_2O_3, ICDD card no. 01-071-1126) with rhombohedral (hexagonal) crystal structure. The addition of 5 wt.% Fe had no considerable effect on XRD pattern, but in samples containing 10–20 wt.% Fe, the only phase added to the products was iron aluminide (Fe_3Al, ICDD card no. 00-045-1203) with a cubic crystal structure. So, reaction products formed in the reactions containing Fe were not as the same as predicted by reaction 2. The lattice parameter of titanium carbide was calculated from the XRD patterns using Brag's equation and Nelson–Riley function [3,25].

$$a = a_0 + a_0 K \prime \frac{1}{2}\left(\frac{\cos^2\theta}{\sin\theta} + \frac{\cos^2\theta}{\theta}\right) = a_0 + K'' f(\theta) \quad \text{Nelson–Riley function} \tag{4}$$

$$a = d_{(hkl)}\left[h^2 + k^2 + l^2\right]^{1/2} \quad \text{Brag equation} \tag{5}$$

where θ is diffraction angle, is the lattice parameter which is determined by Eq. (5) and $_0$ is the true lattice parameter of TiC which is calculated by Eq. (4). Using XRD patterns, we can draw the variations of lattice parameter versus Nelson–Riley function and extrapolate the true lattice parameter at θ = 90. Fig. 6a and b shows Nelson–Riley function diagrams used for calculating lattice parameter of TiC in samples containing different amounts of Fe and variations of synthesized TiC lattice parameters with iron addition, respectively. Also, the lattice parameter of stoichiometric $Ti_{0.5}C_{0.5}$ is indicated in the figure. As can be understood, the lattice parameter of titanium carbide in the sample synthesized without Fe is lower than that of the stoichiometric one and decreases with the increase of Fe content in the reaction. Different literature that used SHS for synthesis of TiC and composites containing this compound showed that during combustion synthesis, carbon content in the TiC is usually lower than stoichiometric and therefore its formulation represented as TiC_{1-x} ($x < 1$) [3,26,27]. Storms [27] indicated that by decreasing carbon content, lattice parameter of TiC falls. So, a possible reason for lower lattice parameter of TiC in the sample with higher Fe may be decreasing carbon of this phase.

Another reason for this phenomenon may be the dissolution of oxygen in the crystal structure of TiC and formation of titanium

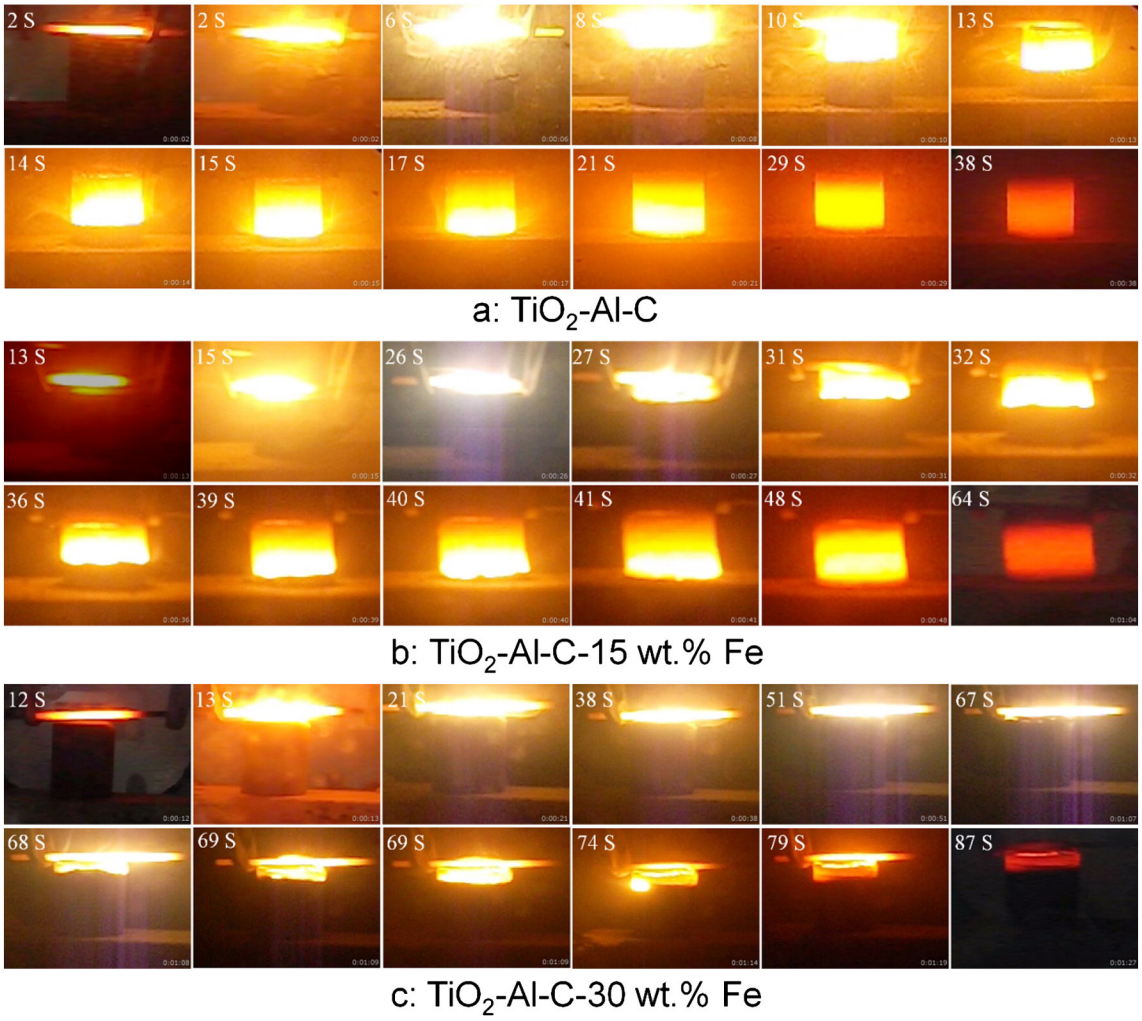

Fig. 3. Reaction initiation, propagation and termination in the samples containing various amounts of Fe.

oxy-carbide. Titanium carbide (TiC) has a NaCl face centered cubic (FCC) crystal structure. TiO also has the same crystal structure of TiC. So, they can form a series of continuous solid solutions like $TiC_{1-x}O_x$ ($0 < x < 1$). Titanium oxy-carbide ($TiC_{1-x}O_x$) is an intermediate product usually observed during carbothermal reduction of TiO_2. Jiang et al. showed that as TiO increases in the titanium oxy-carbide phase, lattice parameter of this phase falls from 0.4324 nm for TiC to 0.4194 for TiO [28].

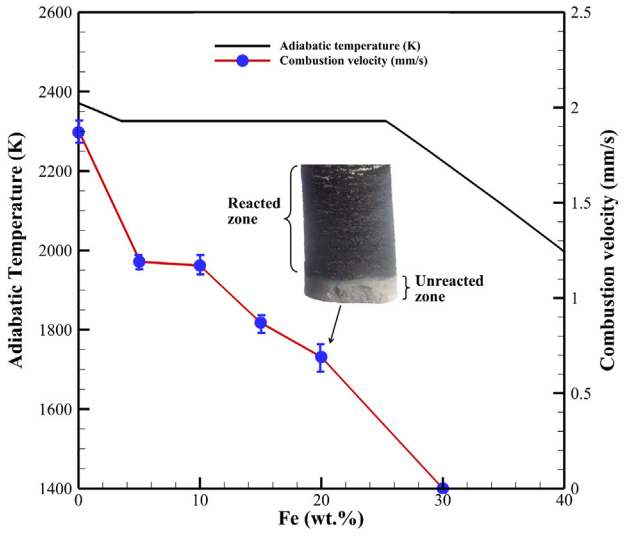

Fig. 4. Simultaneous effects of Fe on combustion velocity and adiabatic temperature of reaction 2.

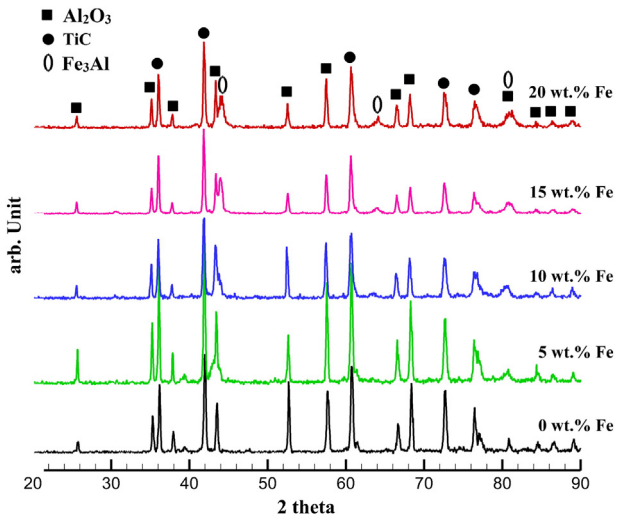

Fig. 5. XRD analysis of samples with 0–20 wt.% Fe.

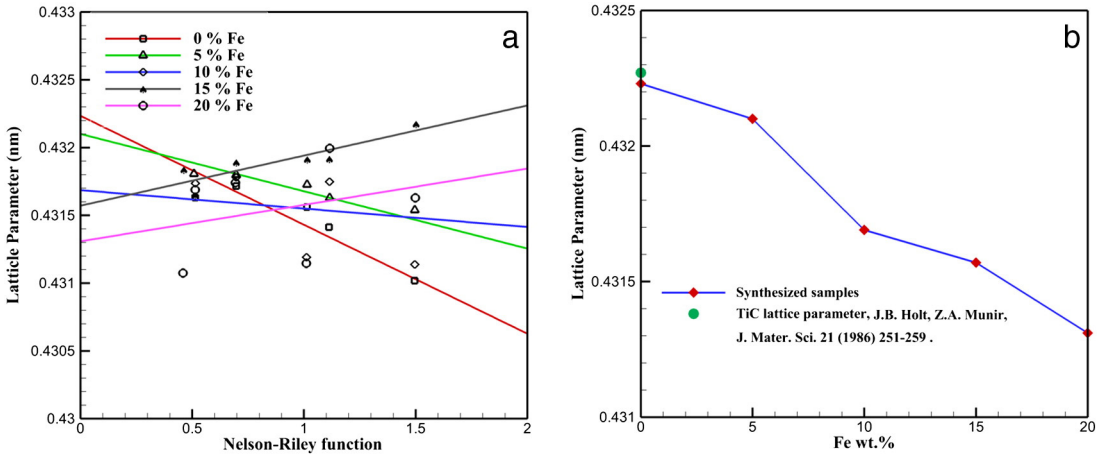

Fig. 6. a: Nelson–Riley function diagram for samples with different Fe contents and b: variations of TiC lattice parameter with Fe additions.

Raman analysis

Raman microscopy is able to determine phases for polymorphic solids at the microscopic level. This is its advantage over conventional X-ray diffraction spectrometry in which the sample volume cannot be too small. Phase identification with Raman spectroscopy uses the characteristic vibration band(s) associated with a certain phase in a solid. This analysis is founded on the Raman scattering of electromagnetic radiation by atoms and molecules. When irradiating materials with electromagnetic radiation of a single frequency, the light will be scattered by molecules elastically and inelastically. The inelastic scattering is called Raman scattering and can be used to determine details of the structure of the molecule or crystal lattice [29].

To study the reaction products more precisely, micro-Raman spectroscopy analysis was performed on different samples. Some Raman spectroscopy analysis on titanium carbide [30,31] reported that the stoichiometric titanium carbide has no Raman active mode and the Raman scattering in this carbide is caused by the disorder induced by carbon vacancy. Fig. 7a–c shows the results of the Raman spectroscopy analysis in the samples containing 0, 10 and 20 wt.% Fe, respectively. In the sample without Fe, five different peaks can be

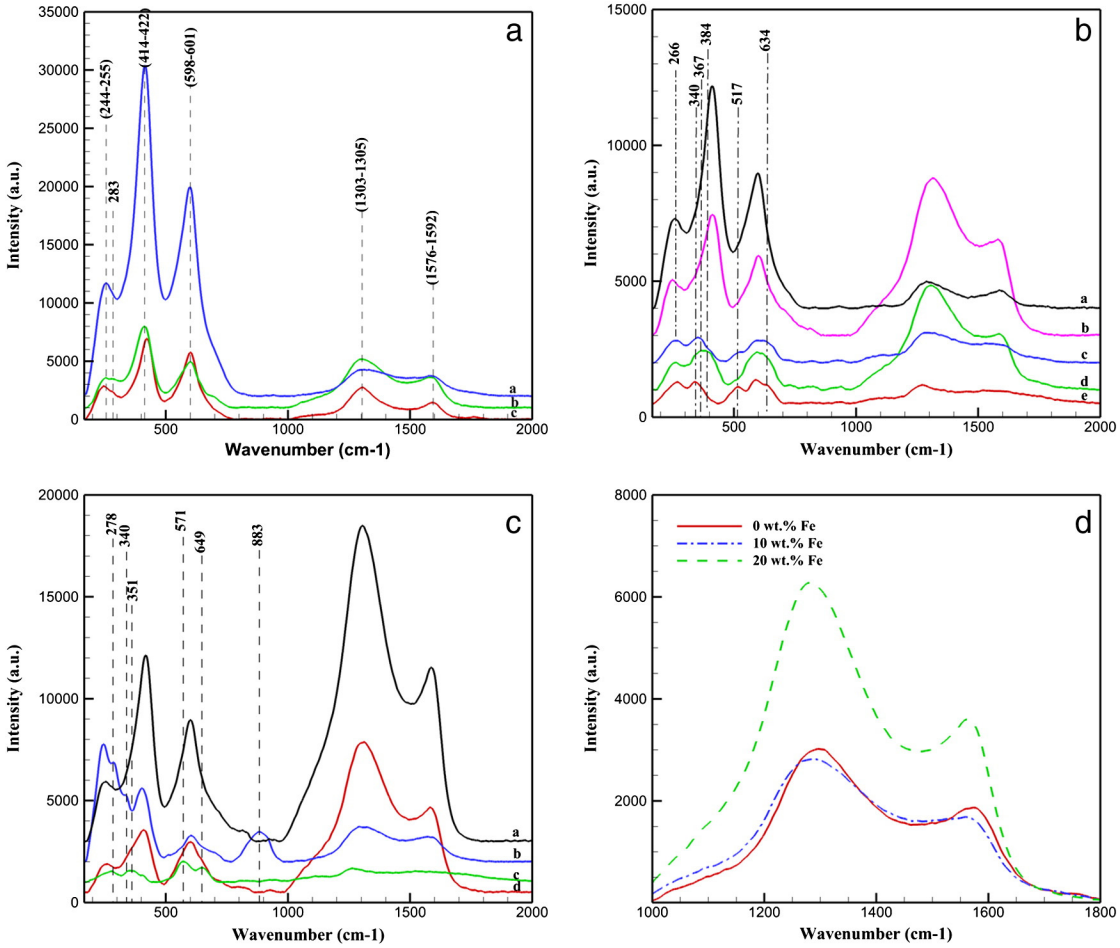

Fig. 7. Raman spectroscopy analysis of samples with a: 0 wt.% Fe, b: 10 wt.% Fe, c: 20 wt.% Fe and d: Raman spectra of TiC in samples with different Fe contents.

observed (Fig. 7a). The first three peaks between 244 and 255, 414 and 422 and 598 and 601 cm^{-1} are related to the titanium carbide, which is almost the same as those reported by Lohse et al. [31] and the two peaks between 1300 and 1600 are related to the un-reacted free active carbon. There is no separate characteristic peak related to Al_2O_3. Cava et al. [32] reported that -Al_2O_3 with a cubic crystal structure has no Raman active mode while α-Al_2O_3 with a hexagonal crystal structure has two Raman active modes with characteristic peaks at 380 and 420 cm^{-1}. As shown by XRD analysis, the synthesized alumina in all samples has a hexagonal crystal structure and thus should have two characteristic peaks. But, it seems that these peaks have overlapped with intense TiC characteristic peak at 420 cm^{-1} and could not be observed in these spectra. The addition of 10 wt.% Fe to the reaction led to the formation of a new peak at 266, some peaks between 340 and 384 cm^{-1} and two new peaks at 517 and 634 cm^{-1}. Also, there is a broad peak between 278 and 351 cm^{-1}, a new peak at 649 cm^{-1} and a broad peak between 680 and 950 cm^{-1} in the sample containing 20 wt.% Fe.

Table 2 shows briefly the characteristic Raman bands of different phases that may be formed after synthesis. By comparing the results of this table with the Raman spectra in Fig. 7a–c, it can be concluded that besides TiC and un-reacted carbon, there is a little TiO_2 with two weak characteristic peaks at 517 and 634–649 cm^{-1}. Also, some peaks between 266 and 384 cm^{-1} and two broad peaks between 550 and 620 cm^{-1} and 680 and 950 cm^{-1} are symptoms related to the formation of titanium oxy-carbide (Ti (C,O)) in the final products. Getting hold of the results of XRD and Raman together, it can be concluded that the addition of Fe to reaction 2 led to the increase of oxygen content in the crystal structure of TiC and formation of titanium oxy-carbide with lower lattice parameter.

In Raman spectroscopy, the intensity of phase characteristic peaks is dependent on its quantity. Fig. 7d compares the mean spectrum of the free carbon in the samples synthesized with different Fe contents. It can be seen that the addition of Fe to the reaction increased the mean intensity and surface area of un-reacted carbon characteristic peaks. So, one can anticipate that the volume fraction of unreacted carbon is higher in the sample with more Fe content.

Microstructural analysis

The SEM microstructures of the fracture surfaces of samples are depicted in Fig. 8. Referable to the presence of considerable amounts of porosity in the final structure of the products, the fracture occurred intergranulary in all samples [8]. The microstructure of the sample with no Fe consists of large Al_2O_3 grains and TiC particle sintered together (Fig. 8a). The addition of 5 wt.% Fe to the reaction changed the morphology of Al_2O_3 from the large plate like grains to slightly finer grains with near spherical morphology. Also, TiC grain size decreased and they became almost spherical in this sample (Fig. 8b). In the sample containing 10 wt.% Fe, the TiC particles became finer, with a particle size between 1 and 5 μm (Fig. 8c and d). It is interesting to notice that there are repeating step on some surfaces of the TiC particles. These steps are characteristics of crystal growth with interface-controlled growth mechanism. Usually, crystal growth in the vapor phase or melt is controlled by three different mechanisms, including diffusion in the melt or vapor, latent heat flow from the crystal-melt interface and reaction at the crystal interface or interface-controlled growth [36]. The interface-controlled growth mechanism is divided into two different categories named continuous and lateral growths. In continuous growth, atoms can attach to the crystal surface at any point of the growing surface. In these conditions the interface grows uniformly. But, lateral growth leads to the movement of a step across the interface and the atoms only can attach to the step. The step height can be one, several or a great number of atom layers (macrosteps) depending on its lateral growth rate and will be higher for a layer with a slower edge growth rate. There are two types of lateral mechanisms, as surface nucleation and screw dislocation. In surface nucleation mechanism, new steps are nucleated on top of each other and form a pyramid-like interface [37]. On the other hand, the screw dislocation model proposed by Hilling and Turnbull [38] puts on that screw dislocations emerge from the growing crystal face and cause the formation of repeating step like an Archimedean spiral [36]. There are some evidences for the formation of two dimensional nuclei on some surfaces of TiC particles. So, it seems that surface nucleation-interface controlled growth mechanism is the growth controlling mechanism of TiC particles in this sample. Fig. 8e and f shows the different magnifications of the fracture surface in the sample containing 15 wt.% Fe. It can be seen that TiC particle size decreased slightly, but their morphology is transformed into cubical particles with faceted morphology. According to the statements of Kirkpatrick faceted [36], taught there is not a theoretical justification, Cahn et al. suggested that crystals with non-faceted morphology grow by continuous mechanism while crystals with faceted morphology, grow with lateral growth mechanism. Choi and Rhee [13] suggested that the aluminothermic reduction of TiO_2 is controlled by the diffusion of carbon through solid TiC. So, it seems that the addition of Fe to the reaction changed the mechanism controlling the growth of TiC particles from diffusion controlled growth in the sample without Fe to lateral growth interface controlled mechanism for samples containing Fe higher that 10 wt.%. The fracture surface of a sample containing 20 wt.% Fe is shown in Fig. 8g and h. The addition of higher Fe to the reaction caused the decrease of TiC particle size and porosity volume fraction in this sample.

Table 2
Raman characteristic peaks of different phases.

Compound	Characteristics Raman peak (cm^{-1})				
TiC [31]	260	420	605		
Carbon [31]	1320	1590			
α-Al_2O_3 [32]	380	420			
TiO_2 [33]	144	197	396	519	639
Ti(C,O) [34]	300–390	560–620	690–830		
Ti_2O_3 [35]	269				

Discussion

The aim of the present study was to investigate the outcome of iron addition on SHS characteristics and phases that formed during combustion synthesis of the TiO_2–Al–C system. The considered reaction is as follows:

$$3TiO_2 + 4Al + 3C + xFe \rightarrow 3TiC + 2Al_2O_3 + xFe \quad (2).$$

The calculation of theoretical adiabatic temperature for this reaction suggests that iron can be added to this reaction up to 53.13 wt.% and it will remain self-sustaining according to Merzhanov criterion [8]. But, first experimental investigations showed that in the sample containing 30 wt.% Fe, the reaction only happened in a thin top surface layer of the compacted powder and then it ended which means that the reaction does not propagate in the SHS mode for this sample. These results are inconsistent with the theoretical results. XRD analysis indicated that the reaction products consist of TiC, Al_2O_3 and Fe_3Al intermetallic phases. These reaction products are not the same as the product of reaction 2, because in this reaction it was expected that Fe would not participate in the reaction and act only as a diluent agent. But, experimental results showed that some of the aluminum was reacted with iron to form a Fe_3Al phase. Zarezadeh Mehrizi and co-workers [39] showed that during combustion synthesis of ferrotitanium–Al–C mixture, the reaction of Fe and Al happens in the temperature range of 973–1173 K. This temperature range is lower than that for ignition of the reaction between aluminum and TiO_2 (1173 K) [13]. So, with the reaction of some of Al with Fe, there will be lack of aluminum for complete reduction of all the TiO_2 to Ti. Choi and Rhee [13] indicated that reduction of TiO_2 with aluminum proceeds by way of Ti_3O_5, Ti_2O_3

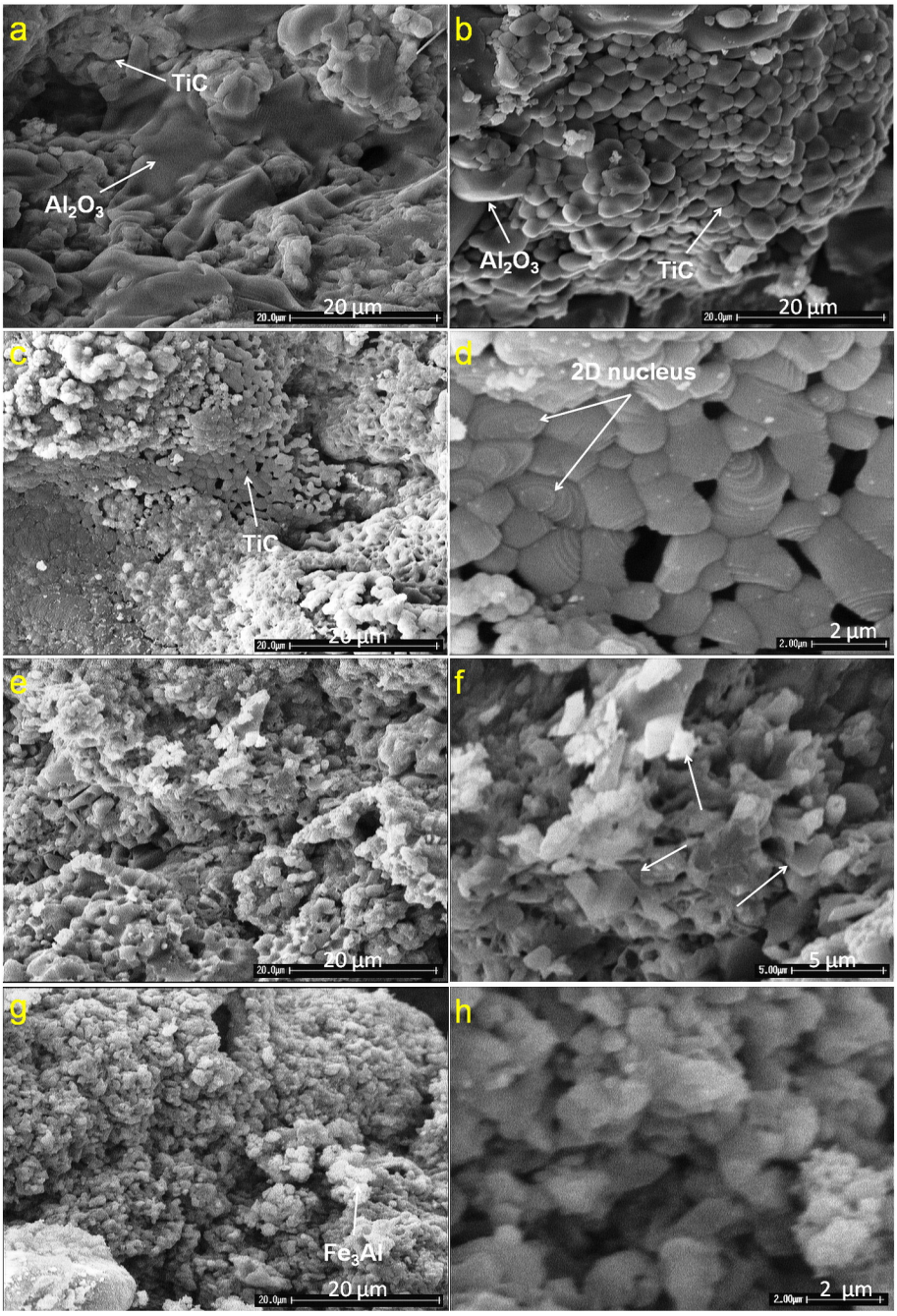

Fig. 8. SEM microstructures of samples with a: 0 wt.% Fe, b: 5 wt.% Fe, c and d: 10 wt.% Fe, e and f: 15 wt.% Fe and g and h: 20 wt.% Fe.

and TiO mid-products to form Ti and Al_2O_3. Similar results were presented by Khoshhal and co-workers [19] and Zou et al. [40] during aluminothermic reduction of ilmenite. Because there was not any peak related to the TiO_2 in the XRD patterns and the characteristic peaks of this phase in the Raman spectra were weak, so it is expected that the quantity of this phase is low in all samples. Therefore, the lack of aluminum for complete reduction of TiO_2 caused partial reduction of it and formation of lower titanium oxide like Ti_3O_5, Ti_2O_3 and TiO and Al_2O_3. Then these oxides reacted with carbon to form oxy-carbide ($TiC_{1-x}O_x$) as indicated by XRD analysis through decreasing of lattice parameter of TiC and characteristic peaks of this phase in Raman spectroscopy results. Comparing the lattice parameter calculated for Ti(C,O) in the sample containing 20 wt.% Fe with that proposed by Jiang et al. [28], it is anticipated that the maximum oxygen content of titanium oxy-carbide (x) will be 0.3 and so the chemical formula of the oxy-carbide is $TiC_{0.7}O_{0.3}$ in this sample. The presence of TiO_2 peaks in the Raman spectra of samples containing 10 and 20 wt.% Fe may be because of this fact that raw materials were not uniform and adding Fe to them raised the distance between TiO_2 and Al particles. So, in some places of the compacts, Al and TiO_2 might not be in contact together and therefore no reduction happened.

In reaction 2, it was expected that all the carbon reacts with Ti to form stoichiometric titanium carbide. But, Raman analysis of the sample with no Fe showed characteristic peaks of un-reacted carbon. In other words, it indicated that in the aluminothermic reduction of TiO_2, all the carbon did not react with the titanium. So, the titanium carbide formed would not be a stoichiometric one and its chemical formula is TiC_x ($x < 1$). This result is in agreement with the difference observed

in Fig. 6 between the lattice parameters of the stoichiometric TiC and that measured for synthesized TiC in the sample with no Fe.

When the amount of Fe added to the reaction increased, more aluminum was used in the reaction with Fe, so the volume fraction of reduced Ti falls. As a result, the quantity of titanium oxide mid-products and the possibility for the formation of titanium oxy-carbide with higher oxygen content and lower lattice parameter increased as shown in Fig. 6. Also, the increase of oxygen in the titanium oxide mid-product and the decrease of combustion temperature with the addition of Fe reduced the amount of carbon participated in the reaction and led to the increase in volume fraction of un-reacted carbon in the final products as indicated by the amplification of carbon peaks in the Raman spectra of samples with higher Fe contents (Fig. 7d). It should be noted that the possibility of reducing the remaining TiO_2 with excess carbon (carbothermal reaction) in the samples containing Fe is low due to the two following reasons: first, according to thermodynamic data, the standard Gibbs free energy of the reaction between TiO_2 and carbon is positive below 1473 K and therefore this reaction proceeds at very high temperatures (1973–2373 K) in argon atmosphere [25]. As indicated in Fig. 1, the adiabatic temperature of the aluminothermic reaction is 2371 K and adding Fe to the reaction decreased it considerably. Usually, the combustion temperature of an SHS reaction is lower than the adiabatic temperature due to the heat loss to the surrounding area [7,8,15]. So, it is expected that as the Fe was added to the reaction, the combustion temperature decreased which lowered the possibility of carbothermic reaction. Second, carbothermal reduction of TiO_2 needs high reaction times (10–24 h) [25]. But, the reaction times for small SHS samples are in the range of seconds to a few minutes. So, one can expect that although this reaction can happen during SHS of the present samples, especially in the samples with lower Fe contents due to their higher combustion temperature, but, the extent of its propagation was not high and therefore the amount of carbon used for carbothermic reduction of TiO_2 was negligible. According to the above Results and Discussion sections, it is expected that the right pass for reaction 2 will be as follows:

$$3TiO_2 + 4Al + 3C + xFe \rightarrow 3Ti\left(C_{1-\frac{x}{6}}O_{\frac{x}{6}}\right) + \left(2-\frac{x}{6}\right)Al_2O_3 + \frac{x}{3}Fe_3Al + \frac{x}{2}C. \quad (6)$$

Fig. 9 shows the effect of Fe on adiabatic temperature of reaction 6 which was estimated using the thermodynamic data of Table 1 with this assumption that at low oxygen content, the thermodynamic properties of titanium oxy-carbide ($TiC_{1-x}O_x$) are the same as those of titanium carbide (TiC). The effect of Fe on adiabatic temperature of reaction 2 is also shown on the figure for comparison. It is observed that the adiabatic temperatures of reaction 6 were 1916 and 1421 K for the samples containing 15 and 20 wt.% Fe which are respectively higher and lower than Merzhanov criterion. So, these new calculated values are consistent with the Merzhanov criterion and experimental observations shown in Fig. 4. As shown earlier in Fig. 4, the reaction is stable for the sample containing 15 wt.% Fe, but, not stable for the sample containing 20 wt.% Fe. So, the Merzhanov criterion is satisfied between these two values as indicated in Fig. 9. It is worse, noting that if 20 wt.% Fe is added to reaction 6, the amount of oxygen (x) in the Ti ($C_{1-x}O_x$) phase will be 0.29. This result is in agreement with the lattice parameter of titanium oxy-carbide purposed by Jiang [28] and that was calculated in Fig. 6.

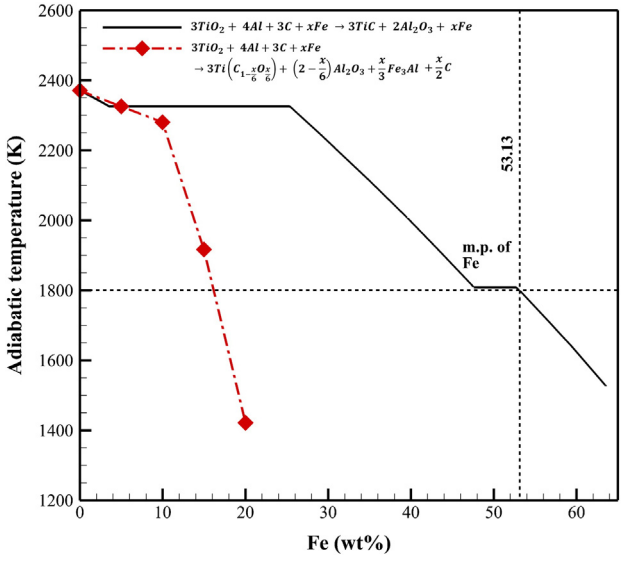

Fig. 9. Effect of Fe on adiabatic temperature of reactions 2 and 6.

From microstructural viewpoint, the addition of Fe to the reaction changed the growth mechanism of the TiC particles from diffusion controlled growth to lateral growth-interface controlled mechanisms. But, the authors think that it needs more investigations which should be considered in the future works.

Conclusion

In the present research, several quantities of Fe were added to the SHS reaction of the TiO_2–Al–C system to fabricate Fe–TiC–Al_2O_3 composite. The main results can be summarized as follows:

1. Thermodynamic calculations predict that if the amount of Fe is lower than 53.13 wt.%, the reaction propagates in the self-sustaining mode. But, experimental data showed that the reaction front became unstable between 15 and 20 wt.% Fe, which was considerably lower than that predicted by thermodynamic data.
2. Phase analysis using XRD and Raman spectroscopy indicated that Fe_3Al, Ti (C,O) and Al_2O_3 with some residual un-reacted carbon were the main products of the synthesis in the samples containing Fe. These products were not the same as those expected earlier.
3. Using Raman spectroscopy analysis, it was demonstrated that all the carbon did not react with Ti in the sample containing no Fe and therefore the C/Ti ratio in the TiC phase was less than unity. This led to a lower lattice parameter for the synthesized TiC in comparison to stoichiometric one. Also, the lattice parameter of Ti (C,O) phase was lower in the samples containing higher Fe, likely as a result of dissolution of higher oxygen in this phase.
4. Microstructural observations showed that additions of Fe changed the growth controlling mechanism of TiC particles.
5. The adiabatic temperatures calculated using the thermodynamic data of the new products for samples containing 15 and 20 wt.% Fe were in conformance with the experimental observations and Merzhanov criterion.

References

[1] Zhu H, Dong K, Wang H, Huang J, Li J, Xie Z. Reaction mechanisms of the TiC/Fe composite fabricated by exothermic dispersion from Fe–Ti–C element system. Powder Technol 2013;246:456–61.
[2] Wang XH, Zhang M, Zou ZD, Song SL, Han F, Qu SY. In situ production of Fe–TiC surface composite coatings by tungsten-inert gas heat source. Surf Coat Technol 2006;200:6117–22.
[3] Razavi M, Rajabi-Zamani AH, Rahimipour MR, Kaboli R, Ostad Shabani M, Yazdani-Rad R. Synthesis of Fe–TiC–Al_2O_3 hybrid nanocomposite via carbothermal reduction enhanced by mechanical activation. Ceram Int 2011;37:443–9.
[4] Zhang W, Zhang X, Wang J, Hong C. Effect of Fe on the phases and microstructure of TiC–Fe cermets by combustion synthesis/quasi-isostatic pressing. Mater Sci Eng A 2004;381:92–4.
[5] Fatemi Nayeri SHR, Vahdati Khaki J, Aboutalebi MR. Implementation of combined mechanical activation and thermal analysis for identification of combustion synthesis mechanism in TiO_2–Al–C system. Iran J Mater Sci Eng 2009–10;6:7–14.
[6] Fatemi Nayeri SHR, Vahdati Khaki J, Aboutalebi MR. The effect of milling conditions on the mechanical alloying and combustion synthesis of TiO_2–Al–C powder mixture. Iran J Mater Sci Eng 2006;3:25–31.

[7] Zou B, Xu J, Wang Y, Zhao S, Fan X, Hui Y, et al. Self-propagating high-temperature synthesis of TiC–TiB_2-based Co cermets from a Co–Ti–B_4C system and fabrication of coatings using the cermet powders. Chem Eng J 2013;233:138–48.
[8] Moore JJ, Feng HJ. Combustion synthesis of advanced materials: part I. Reaction parameters. Prog Mater Sci 1995;39:243–73.
[9] Lee JH, Ko SK, Won CW. Combustion characteristics of TiO_2/Al/C system. Mater Res Bull 2001;36:1157–67.
[10] Amel-Farzad H, Vahdati-Khaki J, Haerian A, Youssefi A. Combustion wave stability in diluted TiO_2/Al/C system in atmospheric air. Solid State Sci 2008;10:1958–69.
[11] Xia TD, Munir ZA, Tang YL, Zhao WJ, Wang TM. Structure formation in the combustion synthesis of Al_2O_3–TiC composites. J Am Ceram Soc 2000;83:507–12.
[12] Bowen CR, Derby B. The formation of TiC/Al_2O_3 microstructures by a self-propagating high-temperature synthesis reaction. J Mater Sci 1996;31:3791–803.
[13] Choi Y, Rhee SW. Reaction of TiO_2–Al–C in the combustion of TiC–Al_2O_3 composite. J Am Ceram Soc 1995;78:986–92.
[14] Saidi A, Chrysanthou A, Wood JV, Kellie JLF. Characteristics of the combustion synthesis of TiC and Fe–TiC composites. J Mater Sci 1994;29:4993–8.
[15] Saidi A, Chrysanthou A, Wood JV, Kellie JLF. Preparation of Fe–TiC composites by the thermal-explosion mode of combustion synthesis. Ceram Int 1997;23:185–9.
[16] Cho CH, Kim DK. Microstructure evolution and isothermal compaction in TiO_2–Al–C combustion reaction. J Mater Synth Process 2002;10:127–34.
[17] Xia TD, Liu TZ, Zhao WJ, Ma BY, Wang TM. Self-propagating high-temperature synthesis of Al_2O_3–TiC–Al composites by aluminothermic reactions. J Mater Sci 2001;36:5581–4.
[18] Zhu H, Jiang Y, Yao Y, Song J, Li J, Xie Z. Reaction pathways, activation energies and mechanical properties of hybrid composites synthesized in-situ from Al–TiO_2–C powder mixtures. Mater Chem Phys 2012;137:532–42.
[19] Khoshhal R, Soltanieh M, Boutorabi MA. Formation mechanism and synthesis of Fe–TiC/Al_2O_3 composite by ilmenite, aluminum and graphite. Int J Refract Met Hard Mater 2014;45:53–7.
[20] Chakraborty SP, Sharma IG, Suri AK, Bose DK. Studies on preparation, characterization and evaluation of properties of Fe_3Al-based intermetallic alloy of composition Fe–16Al–5.44Cr–1Nb–0.5C. J Mater Process Technol 2001;115:413–22.
[21] Desai PD. Thermodynamic properties of selected binary aluminum alloy systems. J Phys Chem Ref Data 1987;16:109–24.
[22] Kubashewski O, Alcock CB. Metallurgical thermochemistry. New York: Pergamon Press; 1979.
[23] Barin I. Thermochemical data of pure substances. 3rd ed. New York: VCH; 1995.
[24] Ma J, Yang J, Bi Q, Liu W. Preparation of an ultrafine-grained Fe–40Al intermetallic compound. Acta Metall Sin 2010;23:50–6.
[25] Sen W, Xu BQ, Yang B, Sun HY, Song JX, Wan HL, et al. Preparation of TiC powders by carbothermal reduction method in vacuum. Trans Nonferrous Met Soc China 2011;21:185–90.
[26] Hajalilou A, Hashim M, Nahavandi M, Ismail I. Mechanochemical carboaluminothermic reduction of rutile to produce TiC–Al_2O_3 nanocomposite. Adv Powder Technol 2014;25:423–9.
[27] Storms EK. The refractory carbides. New York: Academic Press; 1967.
[28] Jiang B, Hou N, Huang S, Zhou G, Hou J, Cao Z, et al. Structural studies of $TiC_{1-x}O_x$ solid solution by Rietveld refinement and first-principles calculations. J Solid State Chem 2013;204:1–8.
[29] Leng Y. Materials characterization. Singapore: John Wiley & Sons; 2008.
[30] Klein MV, Holy JA, Williams WS. Raman scattering induced by carbon vacancies in TiC_x. Phys Rev B 1978;15:1546–56.
[31] Lohse BH, Calka A, Wexler D. Raman spectroscopy as a tool to study TiC formation during controlled ball milling. J Appl Phys 2005;97:114912–7.
[32] Cava S, Tebcherani SM, Souza IA, Pianaro SA, Paskocimas CA, Longo E, et al. Structural characterization of phase transition of Al_2O_3 nanopowders obtained by polymeric precursor method. Mater Chem Phys 2007;103:394–9.
[33] Choi HC, Jung YM, Kim SB. Size effects in the Raman spectra of TiO_2 nanoparticles. Vib Spectrosc 2005;37:33–8.
[34] Hassan M, Rawat RS, Lee P, Hassan SM, Qayyum A, Ahmad R, et al. Synthesis of nanocrystalline multiphase titanium oxycarbide (TiC_xO_y) thin films by UNU/ICTP and NX2 plasma focus devices. Appl Phys A 2008;90:669–77.
[35] Chappé JM, Fernandes AC, Moura C, Alves E, Barradas NP, Martin N, et al. Analysis of multifunctional titanium oxycarbide films as a function of oxygen addition. Surf Coat Technol 2012;206:2525–34.
[36] Kirkpatrick RJ. Crystal growth from the melt: a review. Am Mineral 1975;60:798–804.
[37] Fredriksson H, Akerlind U. Solidification and crystallization processing in metals and alloys. United Kingdom: John Wiley & Sons; 2012.
[38] Hilling WB, Turnbull D. Theory of crystal growth in pure undercooled liquids. J Phys Chem 1956;24:914.
[39] Zarezadeh Mehrizi M, Saidi A, Shamanian M, Eslami HR. Combustion synthesis of Fe–Al/TiC composite powders and effect of Al content on its characteristics. Powder Metall 2011;54:400–3.
[40] Zou Z, Wu Y, Yin C, Li X. Preparation of Fe–Al intermetallic/TiC–Al_2O_3 ceramic composites from ilmenite by SHS. J Wuhan Univ Technol Mater Sci Ed 2007;22:706–9.